Available online at www.sciencedirect.com
SCIENCE DIRECT®
ELSEVIER
International Journal of Thermal Sciences 43 (2004) 331–338
International Journal of Thermal Sciences
www.elsevier.com/locate/ijts

Constructal thermal optimization of an electromagnet

Louis Gosselin, Adrian Bejan *

Department of Mechanical Engineering and Materials Science, Box 90300, Duke University, Durham, NC 27708-0300, USA

Received 12 December 2002; accepted 21 August 2003

Abstract

This paper addresses the fundamental problem of optimizing the geometry of an electromagnet by maximizing at the same time its magnetic performance and thermal performance. The solenoid has a cylindrical shape and a uniform current density. Cooling discs made of high thermal conductivity material are inserted in the coil to collect the heat generated by Joule heating. The collected heat is evacuated to the ambient. For a given magnetic performance and volume, the maximum temperature inside the electromagnet is minimized by selecting the shape of the coil (length and outer radius), the number of cooling discs, and the amount of high thermal conductivity material. The two objectives pursued in this geometric optimization (magnetic and thermal) show that the constructal design method can be extended to the generation of architecture for multi-objective systems.

Keywords: Constructal; Electromagnet; Cooling of electronics; Geometry; Thermal design

1. Introduction

Electromagnets are an integral feature of the technological reality. They are essential in an extremely wide variety of applications, and, as a consequence, their design feels the same pressures that rule all of engineering today: miniaturization, compactness and high-density of function served. In the case of electromagnets, the push toward high density means high magnetic fields, low power dissipation, lightweight, and no overheating (safety). In particular, the internal temperature is central for efficient operation, and for preventing the mechanical collapse of the electromagnet.

These objectives are summarized well by Herlach's [1] recent statement that "what is needed in the first place are better materials, good designs and fresh ideas". Efforts have been made in the past to optimize the shape of the solenoid from the magnetic point of view, i.e., to produce higher magnetic field with less power and volume of conductor [2,3]. More recently, Morgan [4] presented a design approach to minimize the weight of the solenoid. However, the heat transfer aspect was not taken into account in these optimizations.

In this paper we propose a constructal approach to the design of electromagnets. This approach addresses the heat transfer objective, which is similar to the objective pursued in the cooling of high-density electronic packages [5,6]. We pursue a geometry that minimizes the hot spot temperature subject to the finite-size constraints detailed in the text. There is more than one reason for considering this approach. First, the hot spot temperature must be below a certain temperature, for example, below the melting point of the conductors and the thermal limit of structural materials. Second, the electrical resistivity increases with the temperature, leading to higher power dissipation. Third, the mechanical strength of the solenoid decreases as the temperature of the structure increases. In sum, heat transfer and geometry play key roles in the quest for high-density and light-weight electromagnets.

2. Electromagnetism

Fig. 1 shows the front and side views of the solenoid. A wire is wound in many layers around a cylindrical space of radius r_0. Even though other shapes can be contemplated for maximizing the magnetic field, we limit the discussion to a cylindrical coil. The current density inside the wire generates a one-dimensional magnetic field on the axis of symmetry of the coil. We consider the solenoid as a continuous medium in

* Corresponding author.
E-mail address: dalford@duke.edu (A. Bejan).

1290-0729/$ – see front matter
doi:10.1016/j.ijthermalsci.2003.08.004

Nomenclature

B_0	magnetic induction at the center of the coil	T
D	half-thickness of a cooling disc	m
G	dimensionless magnetic parameter	
j	current density	$A \cdot m^{-2}$
k_0	low thermal conductivity	$W \cdot m^{-1} \cdot K^{-1}$
k_1	high thermal conductivity	$W \cdot m^{-1} \cdot K^{-1}$
L	half-length of the coil	m
n	number of cooling discs	
P	total power dissipated	W
q'''	volumetric heat source	$W \cdot m^{-3}$
$\tilde{q}$	dimensionless volumetric heat source	
r	radial position	m
r_0	inner radius	m
r_1	outer radius	m
T	temperature	K
T_0	sink temperature	K
V	solenoid volume	m^3

Greek symbols

θ	dimensionless temperature	
ϕ	fraction of the volume occupied by the discs	
ρ	electrical resistivity	$W \cdot m \cdot A^{-2}$

Subscripts

max	maximum
opt	optimal

Superscript

$(\tilde{\ })$	dimensionless parameters

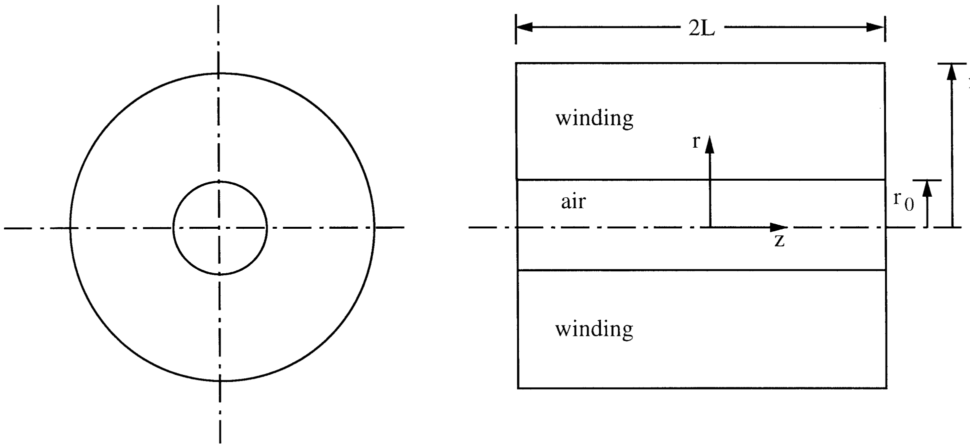

Fig. 1. The main features of solenoid geometry.

which the current density j is constant. The inner and outer radii of the coil are r_0 and r_1, and the axial length is $2L$. In practice, the inner radius is set by the application in which the solenoid is used, and so is the magnetic field that is to be achieved inside the solenoid.

The magnetic induction is maximum at the origin ($z = r = 0$), and at that position is given by [7]

$$B_0 = 0.2\pi j \int_{-L/2}^{L/2} \left(\int_{r_0}^{r_1} \frac{r^2\,dr}{(r^2+z^2)^{3/2}} \right) dz \tag{1}$$

For the purpose of the present demonstration, we will consider that the magnetic induction B_0 is fixed. It represents the magnetic induction that our design must be able to produce for the application of interest. The power dissipated by the electric current used to produce the magnetic field is

$$P = 2\pi\rho j^2 \int_{-L/2}^{L/2} dz \int_{r_0}^{r_1} r\,dr \tag{2}$$

where ρ is the electrical resistivity of the material. Eqs. (1) and (2) can be combined to obtain

$$B_0 = \left(\frac{P}{\rho r_0}\right)^{1/2} G\left(\frac{r_1}{r_0}, \frac{L}{r_0}\right) \tag{3}$$

The function G depends only on geometry: for the case of a constant current density it is given by [7]

$$G = 0.2\left(\frac{2\pi\widetilde{L}}{\tilde{r}_1^2 - 1}\right)^{1/2} \ln\frac{\tilde{r}_1 + (\widetilde{L}^2 + \tilde{r}_1^2)^{1/2}}{1 + (\widetilde{L}^2 + 1)^{1/2}} \tag{4}$$

where

$$(\tilde{r}_1, \widetilde{L}) = \frac{(r_1, L)}{r_0} \tag{5}$$

The G function has been maximized in literature [7,8]. The maximum is $G_{max} = 0.179$, and occurs at $\tilde{r}_{1,opt} = 3.1$ and $\widetilde{L}_{opt} = 1.9$. These geometric features correspond to a dimensionless volume of $\widetilde{V} = 51.4$, where $\widetilde{V}$ has been defined as

$$\widetilde{V} = \frac{V}{r_0^3} = \pi\widetilde{L}(\tilde{r}_1^2 - 1) \tag{6}$$

Fig. 3 shows a constant-G curve in the geometry space. For a fixed power input P, Eq. (3) shows that all the points of the constant-G curve represent designs producing the same magnetic field. The challenge is to find which of these designs is best from the thermal point of view.

3. Heat transfer

Several options are available for cooling the electromagnet effectively. In this paper we examine the use of high thermal conductivity cooling discs of thickness $2D$, as illustrated in Fig. 2. The discs are transversal and separate the solenoid into sub-coils. No current passes through the discs. Their function is simply to collect the heat generated in the solenoid, and to lead it to the exterior. At first, the fraction of the volume occupied by the discs is known and fixed by

$$\phi = \frac{Dn}{L} \tag{7}$$

where n is the number of discs. Most of the volume must be filled by the winding, as required by the drive toward compactness, therefore $\phi \ll 1$. This means that the presence of the discs does not affect significantly the magnetic field, Eq. (1).

Most of the generated heat is transported outside the coil through the inserts. Recognizing that fact, we assume that all the boundaries are adiabatic, except the exposed external surfaces of the discs, which serve as heat sinks, and where the temperature is fixed at T_0. The equation for heat conduction in cylindrical coordinates is

$$\frac{\partial^2 T}{\partial z^2} + \frac{1}{r}\frac{\partial}{\partial r}\left(r\frac{\partial T}{\partial r}\right) + \frac{\rho}{k} j^2 = 0 \tag{8}$$

The thermal conductivity k is set equal to k_0 in the winding, and to k_1 in the cooling discs. Even though the thermal conductivity of typical winding materials is relatively high, for the sake of the present discussion, the conductivity of the inserts is considered to be much larger, $k_1/k_0 \gg 1$. It is quite likely that due to imperfect compactness, the air pockets in the winding will reduce the conductivity k_0. The heat source term in Eq. (8) is related to the fixed power input, Eq. (2).

The heat transfer analysis consists of determining the temperature field for many solenoid shapes, and calculating the hot spot temperature for each shape. A simple analysis can be used at this stage. Consider the case where only one cooling disc is inserted in the coil, $n = 1$. The hot spot is located at the inner radius r_0, and at the maximum axial distance from the cooling disc (Fig. 2). Because the thermal conductivity ratio k_1/k_0 is much greater than one, it makes sense to assume that in the lower conductivity material (the winding) heat flows axially. The heat flow continues radially through the disc, and reaches the heat sink. This unidimensionality of the heat flow in the two sections of the magnet (winding and cooling discs) would also be present if the cooling discs were to be replaced by a more refined cooling technique (for example, water cooled discs). Along the k_0 path, heat flows according to

$$\frac{d^2 T}{dz^2} = \frac{q'''}{k_0} \tag{9}$$

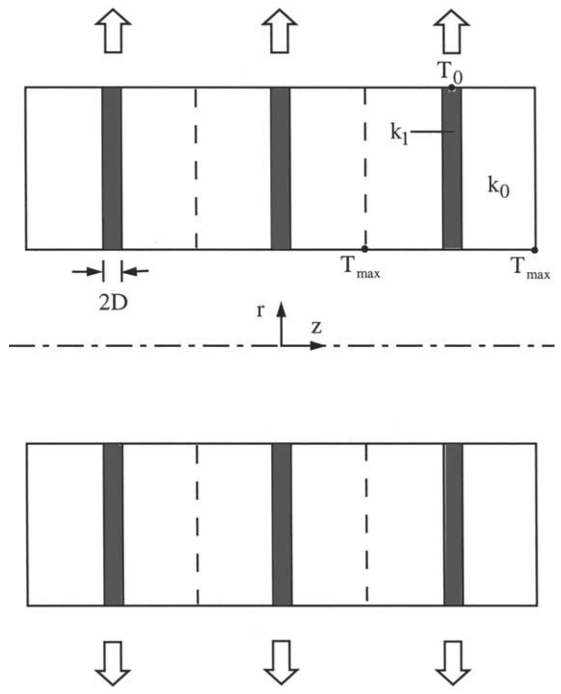

Fig. 2. Solenoid cooled by transversal discs with high thermal conductivity.

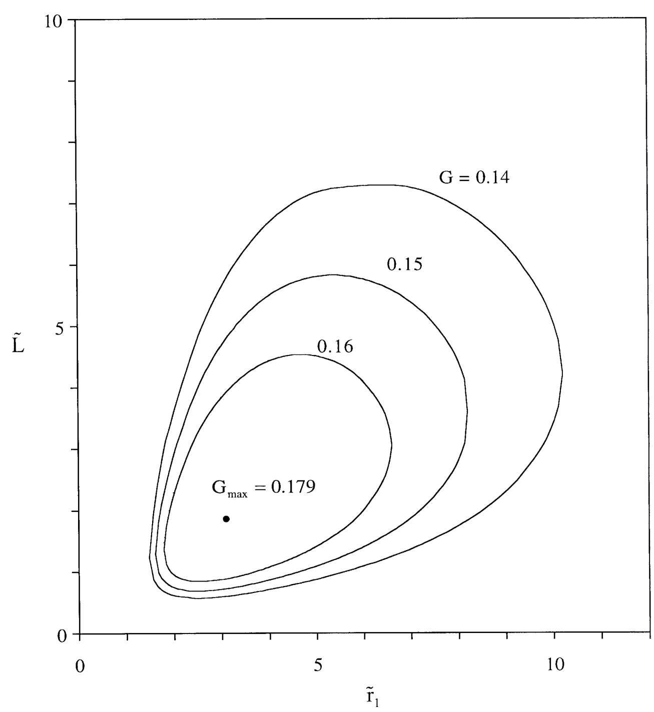

Fig. 3. The locus of designs with constant G in the geometry space $(\tilde{r}_1, \tilde{L})$.

with the boundary condition

$$\frac{dT}{dz} = 0 \quad \text{at } z = L \tag{10}$$

Writing T_c for the temperature in the cooling disc at r_0, we obtain

$$T_{max} - T_c = \frac{q''' L^2}{2k_0} \tag{11}$$

The equation for radial heat conduction through the k_1 material is

$$k_1 D \frac{1}{r}\frac{d}{dr}\left(r\frac{dT}{dr}\right) = Lq''' \tag{12}$$

with the boundary condition

$$\frac{dT}{dr} = 0 \quad \text{at } r = r_0 \tag{13}$$

By solving Eq. (12), we obtain the temperature difference between the inner and outer radii of the disc,

$$T_c - T_0 = \frac{q''' L r_0^2}{4k_1 D}\left[\left(\frac{r_1}{r_0}\right)^2 - 1\right] - \frac{q''' L r_0^2}{2k_1 D}\ln\left(\frac{r_1}{r_0}\right) \tag{14}$$

The temperature difference between the hot spot and the sink is thus the sum of Eqs. (11) and (14),

$$\Delta\widetilde{T}_{max} = \frac{T_{max} - T_0}{P/(r_0 k_0)} = \frac{\widetilde{L}}{2\pi n^2(\tilde{r}_1^2 - 1)} + \frac{1}{2\pi\phi\tilde{k}\widetilde{L}}\left(\frac{1}{2} - \frac{\ln\tilde{r}_1}{\tilde{r}_1^2 - 1}\right) \tag{15}$$

where $\tilde{k} = k_1/k_0 \gg 1$, and the volumetric heat source q''' has been replaced by P/V. The number of discs (n) appears now in Eq. (15).

4. Combining heat transfer with electromagnetism

Fig. 4 shows how the hot spot temperature varies along the constant-G curve, for several n. There is a minimum in every case (marked by a small circle in Fig. 4), and this minimum is a function of n. These minima are reported in Fig. 5. Note that even though the magnetic induction is only 84% of the magnetic induction produced by the electromagnet of optimal shape ($G = 0.15$ instead of $G_{max} = 0.179$), the decrease in the hot spot temperature is relatively larger. The dimensionless hot spot temperature is only 67% of the value for the solenoid of optimal shape.

At this point, we note that the optimized solenoid occupies a much larger volume than the solenoid optimized only from a magnetic point of view. For example, for the case $n = 1$ the optimal outer radius and length of the solenoid optimized with the previous analysis are found to be 8.1 and 4.3, respectively. These dimensions correspond to a dimensionless volume of $\widetilde{V} = 872.8$, which compares unfavorably with the volume of the solenoid optimized from the magnetic point of view only, $\widetilde{V} = 51.4$ (Section 2). There is

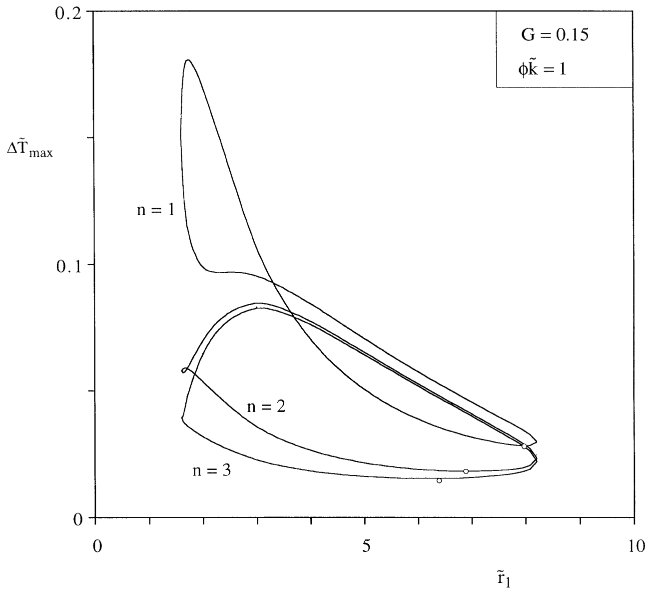

Fig. 4. The behavior of the hot spot temperature when the G and $\phi\tilde{k}$ parameters are fixed.

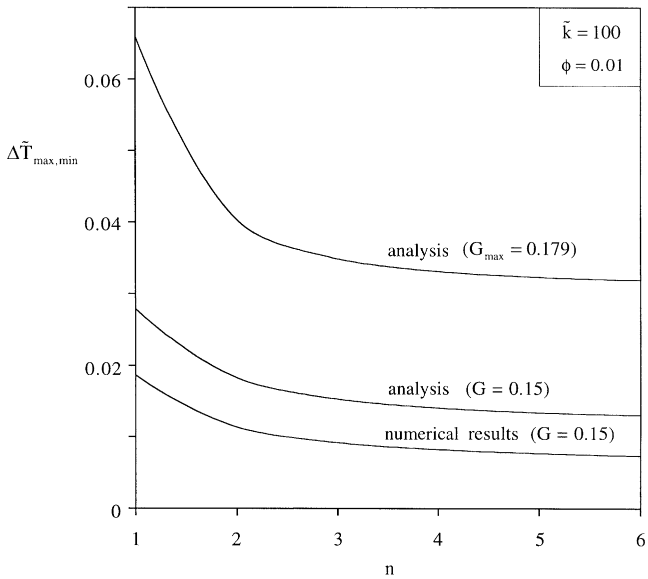

Fig. 5. Comparison between the numerical and analytical results for the hot spot temperature.

one order of magnitude difference between the two volumes. This aspect is discussed in more detail in Section 6. Note further that the hot spot temperature decreases as the number of discs increases. The downside of this is that a more complex solenoid would have to be built.

5. Numerical optimization

The preceding analysis is valid in the limit $\tilde{k} \gg 1$ and $\phi \ll 1$. We also performed a numerical simulation and optimization without the $\tilde{k}$ and ϕ assumptions, and we compared the results with those of Section 4. The dimensionless equation for conduction is

$$\frac{1}{\tilde{r}}\frac{\partial}{\partial \tilde{r}}\left(\tilde{r}\frac{\partial \theta}{\partial \tilde{r}}\right)+\frac{\partial^2\theta}{\partial \tilde{z}^2}+\frac{\tilde{q}}{\tilde{k}}=0 \tag{16}$$

The dimensionless temperature and heat generation rate are

$$\theta=\frac{T-T_0}{P/(r_0k_0)} \tag{17}$$

$$\tilde{q}=\frac{1}{\widetilde{V}} \tag{18}$$

The total power dissipated in the coil, P, which is proportional to the volumetric heat generation rate, q''', has been used to non-dimensionalize the temperature. The heat generation term is equal to zero in the spaces occupied by the high conductivity discs. All the boundaries are adiabatic, except for the outer surfaces of the discs, which are in contact with a temperature reservoir at $\theta = 0$. Eq. (16) was solved using a finite elements code [9]. The grid employed consists of 85 nodes in the axial direction, and 60 nodes in the radial direction. It was found that further grid doubling results in changes smaller than 1% in the dimensionless hot spot temperature. Because the temperature profile is symmetric about the disc midplane, only half of the conducting domain between two consecutive discs was modeled numerically.

The numerical results for $G = 0.15$ are compared with the analytical results in Fig. 5. The agreement between the two curves is adequate in view of the order-of-magnitude character of the analysis. The qualitative trends are the same, analytically and numerically.

The geometric features of the optimal design obtained numerically ($\tilde{r}_{1,\mathrm{opt}}$, $\widetilde{L}_{\mathrm{opt}}$, $\widetilde{V}_{\mathrm{opt}}$) are reported in Fig. 6. As the number of inserted discs increases, the optimal electromagnet becomes thinner and longer. In other words, the optimal outer radius of the electromagnet is a decreasing function of n, while its length is an increasing function of n. The numerical results also confirm a trend outlined by the analysis of Section 4: even though the volume of the optimized electromagnet tends to diminish as n increases, it still remains one order of magnitude greater than the volume for $G = G_{\max}$.

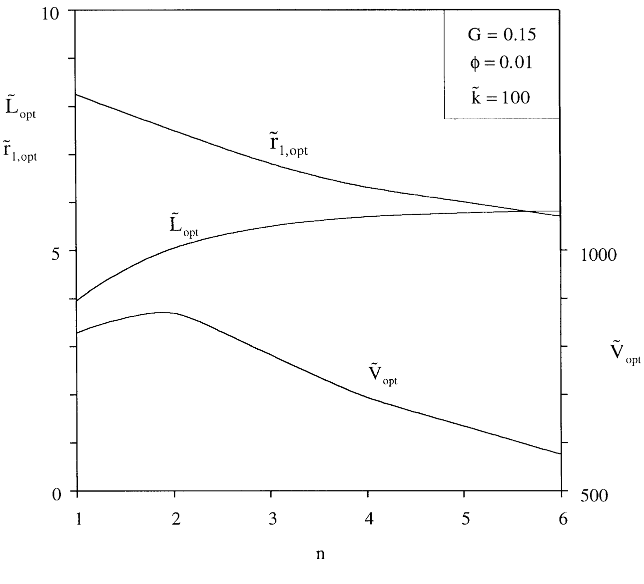

Fig. 6. Optimal geometry for a specified electromagnetic performance (G).

6. Constant volume

The results reported in Section 4 showed that the solenoid optimized thermally and electromagnetically is considerably larger than the winding optimized solely from the electromagnetic point of view. In practice, the volume, amounts of materials and weight are additional constraints. Fixing the amount of electrical conductor is equivalent to fixing the volume of the coil. In this section, we propose to fix the coil volume,

$$\widetilde{V}=\pi\left(\tilde{r}_1^2-1\right)\widetilde{L} \tag{19}$$

This new constraint reduces the number of designs that provide the same magnetic field. Previously, all the points on a constant-G curve represented shapes that were magnetically equivalent. Now, for fixed volume, G-parameter and power input, only two shapes are equivalent from the electromagnetic point of view. These designs are located at the intersection of the constant-G and constant-V curves in the $\tilde{r}_1$–$\widetilde{L}$ plane. See points A and B in Fig. 7.

For a given $\widetilde{V}$ and n, the point with the lowest $\Delta\widetilde{T}_{\max}$ corresponds to the best design. There are two design types, A (thin and long solenoid), and B (thick and short). The optimal design for $n = 1$ is of type B, while for $n \geqslant 2$ the optimal design is of type A. The analytical and numerical results for the optimal designs (A or B) are reported in Fig. 8.

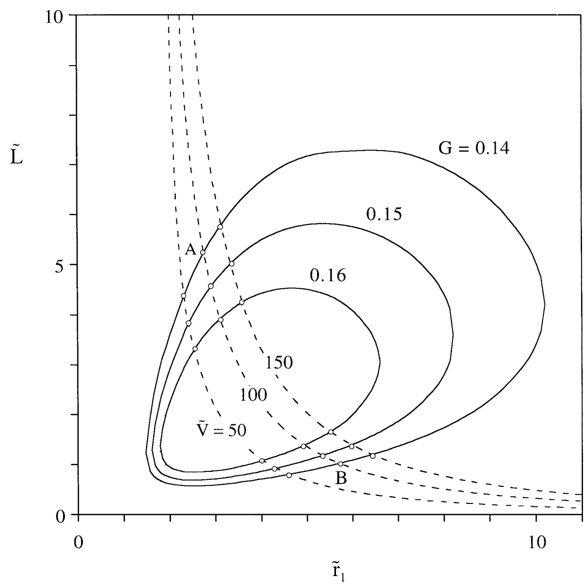

Fig. 7. Designs (A, B) with specified electromagnetic performance (G) and volume ($\widetilde{V}$).

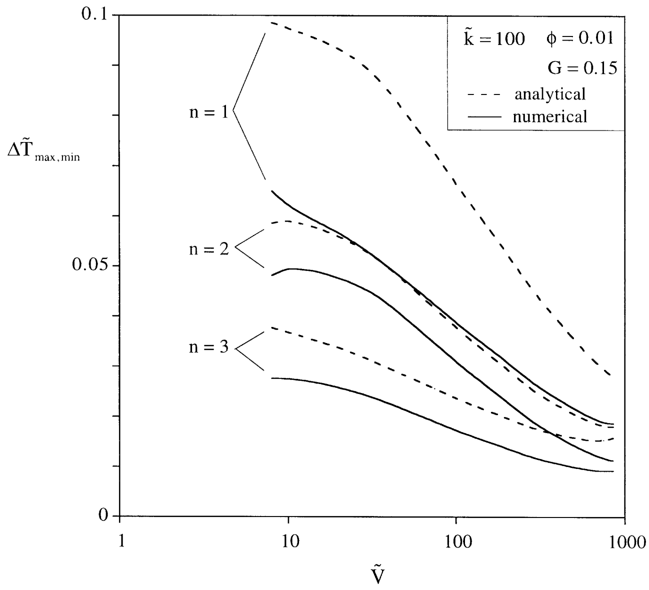

Fig. 8. The effect of the specified volume on the hot-spot temperature at (constant G and ϕ).

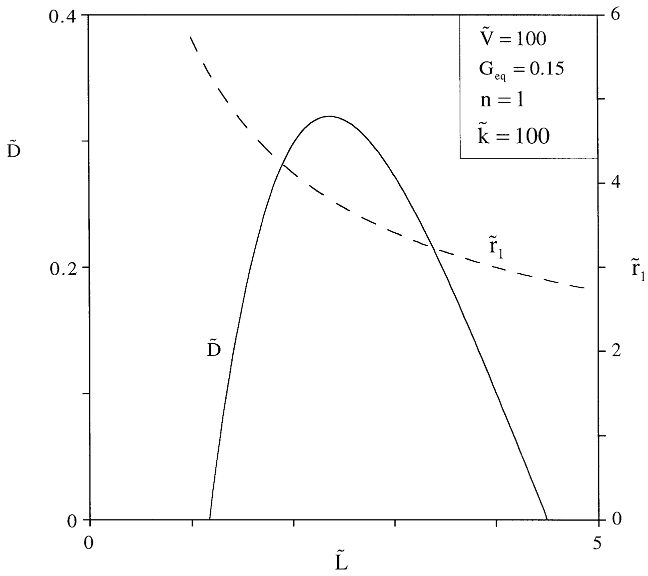

Fig. 9. The relation between $\tilde{r}_1$, $\widetilde{L}$ and $\widetilde{D}$ when the volume occupied by the discs is taken into account in the calculation of G.

7. Optimal amount of high thermal conductivity material

The preceding formulation was based on the assumption that ϕ is much smaller than one. Accordingly, the insertion of discs in the solenoid did not affect the magnetic field. The G parameter was particularly simple in that case.

Now, we propose to optimize the amount of high conductivity material as well. This can be done by taking into account the presence of the cooling discs when calculating the G parameter. Here is why an optimal amount of k_1 material must exist. If this amount increases, the hot spot temperature decreases. On the other hand, because the high-conductivity material does not contribute to the magnetic field, a design with a high ϕ value will not be able to achieve the required (high) magnetic field. There must be a trade-off, where the amount of high conductivity materials is large enough to cool the coil, and small enough to produce a high magnetic field.

Let us start with the simple case $n = 1$. It can be shown that when the cooling discs are taken into account, the equivalent G factor is a function of $\widetilde{L}$, $\widetilde{D}$ and $\tilde{r}_1$ [7]:

$$G_{\mathrm{eq},\,n=1} = \frac{G_{\widetilde{L}}\widetilde{L}^{1/2} - G_{\widetilde{D}}\widetilde{D}^{1/2}}{(\widetilde{L} - \widetilde{D})^{1/2}} \tag{20}$$

The factors $G_{\widetilde{L}}$ and $G_{\widetilde{D}}$ are given by Eq. (4), namely,

$$G_{\widetilde{L}} = 0.2\left(\frac{2\pi\widetilde{L}}{\tilde{r}_1^2 - 1}\right)^{1/2} \ln\frac{\tilde{r}_1 + (\widetilde{L}^2 + \tilde{r}_1^2)^{1/2}}{1 + (\widetilde{L}^2 + 1)^{1/2}} \tag{21}$$

$$G_{\widetilde{D}} = 0.2\left(\frac{2\pi\widetilde{D}}{\tilde{r}_1^2 - 1}\right)^{1/2} \ln\frac{\tilde{r}_1 + (\widetilde{D}^2 + \tilde{r}_1^2)^{1/2}}{1 + (\widetilde{D}^2 + 1)^{1/2}} \tag{22}$$

It is worth noting that $\widetilde{L}$ and $\widetilde{D}$ are now independent variables, because the percentage of the volume occupied by the disc (ϕ) is not fixed, but must be optimized. The external shape features ($\widetilde{L}$, $\tilde{r}_1$) are linked via the total volume constraint, Eq. (19). Fixing $G_{\mathrm{eq},\,n=1}$, P and $\widetilde{V}$ leaves only one degree of freedom. We choose $\widetilde{L}$ as this degree of freedom.

Fig. 9 shows how $\widetilde{D}$ and $\tilde{r}_1$ vary with $\widetilde{L}$. All the designs of Fig. 9 are equivalent magnetically ($G_{\mathrm{eq},\,n=1} = 0.15$) and have the same mass or volume ($\widetilde{V} = 100$). We want to find out which of these designs performs best from the thermal point of view. To this end, we vary $\widetilde{L}$, and solve Eq. (16) numerically. In this more refined analysis, the dimensionless heat source in Eq. (16) is:

$$\tilde{q} = \frac{1}{\widetilde{V}(1 - n\widetilde{D}/\widetilde{L})} \tag{23}$$

i.e., that the power is dissipated only in the coil material. Fig. 10 shows that there is an optimal $\widetilde{L}$, so that $\Delta\widetilde{T}_{\max}$ reaches a minimum. Fig. 9 delivers the corresponding optimal $\widetilde{D}$ and $\tilde{r}_1$. This design is indicated with a small circle. It is an important result because it means that there is an opportunity to take into account simultaneously the magnetic, thermal and volume aspects in the optimization of an electromagnet.

Fig. 11 shows how the minimized hot spot temperature varies with $\widetilde{V}$ and $G_{\mathrm{eq},\,n=1}$. Each point on these curves is the result of the optimization procedure described above. The lighter (small-$\widetilde{V}$) and high-G coils are the worst thermally. The corresponding ϕ_{opt}, $\widetilde{L}_{\mathrm{opt}}$ and $\tilde{r}_{1,\mathrm{opt}}$ values are reported in Figs. 12 and 13.

We also performed the analysis for $n > 1$. The corresponding equivalent G factor for an odd or even number of discs is given respectively by

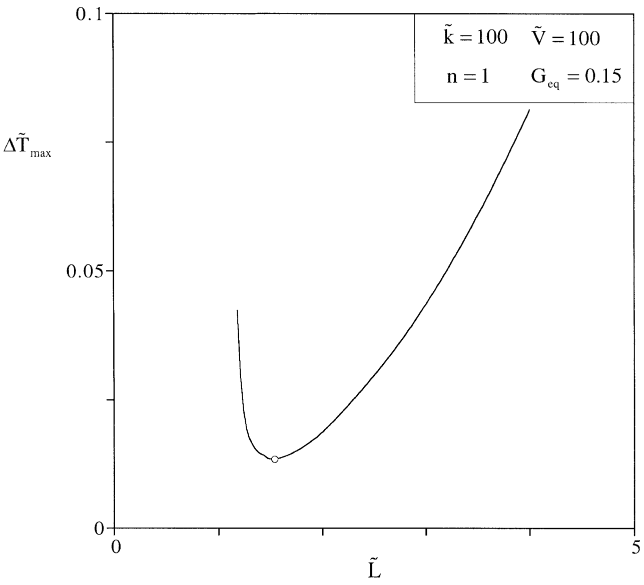

Fig. 10. The effect of $\widetilde{L}$ on the hot-spot temperature when G and $\widetilde{V}$ are fixed.

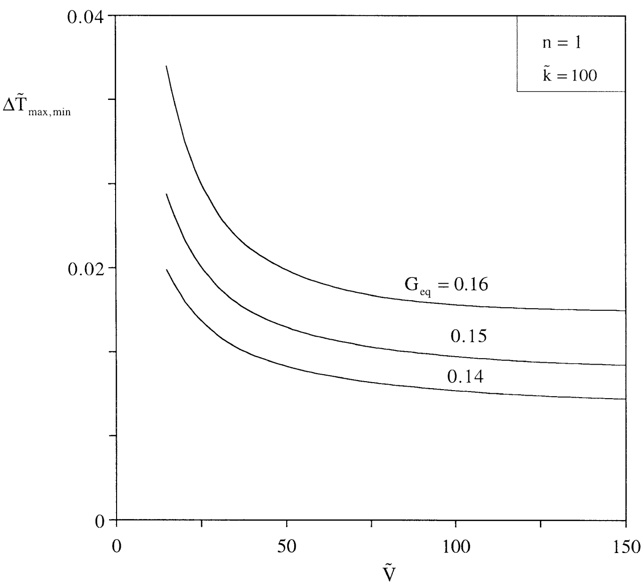

Fig. 11. The effect of G and $\widetilde{V}$ on the minimized hot-spot temperature.

$$G_{\mathrm{eq},\,n\,\mathrm{odd}} = \frac{1}{(\widetilde{L}-n\widetilde{D})^{1/2}}\Bigg[G_{\widetilde{L}}\widetilde{L}^{1/2} - G_{\widetilde{D}}\widetilde{D}^{1/2} + \sum_{i=1}^{(n-1)/2}\Bigg(G_{(2i\widetilde{L})/n-\widetilde{D}}\left(\frac{2i\widetilde{L}}{n}-\widetilde{D}\right)^{1/2} - G_{(2i\widetilde{L})/n+\widetilde{D}}\left(\frac{2i\widetilde{L}}{n}+\widetilde{D}\right)^{1/2}\Bigg)\Bigg] \tag{24}$$

$$G_{\mathrm{eq},\,n\,\mathrm{even}} = \frac{1}{(\widetilde{L}-n\widetilde{D})^{1/2}}\Bigg[G_{\widetilde{L}}\widetilde{L}^{1/2} + \sum_{i=1}^{n/2}\Bigg(G_{((2i-1)\widetilde{L})/n-\widetilde{D}}\left(\frac{(2i-1)\widetilde{L}}{n}-\widetilde{D}\right)^{1/2} - G_{((2i-1)\widetilde{L})/n+\widetilde{D}}\left(\frac{(2i-1)\widetilde{L}}{n}+\widetilde{D}\right)^{1/2}\Bigg)\Bigg] \tag{25}$$

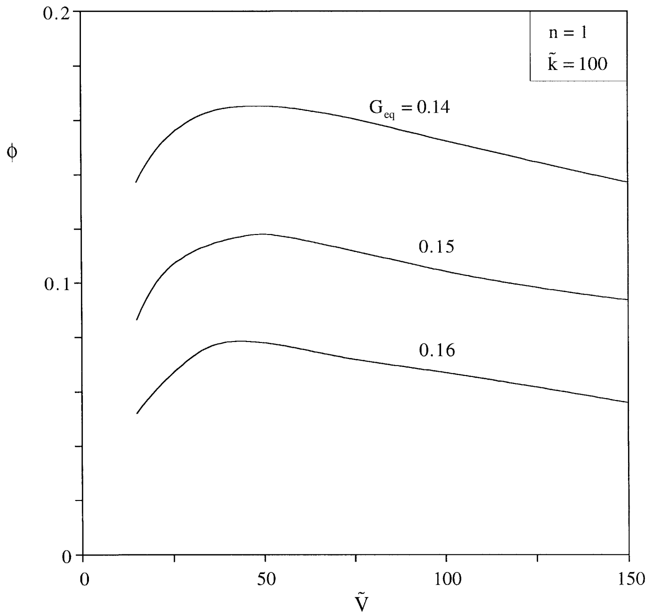

Fig. 12. The optimized fraction of the volume occupied by the cooling discs.

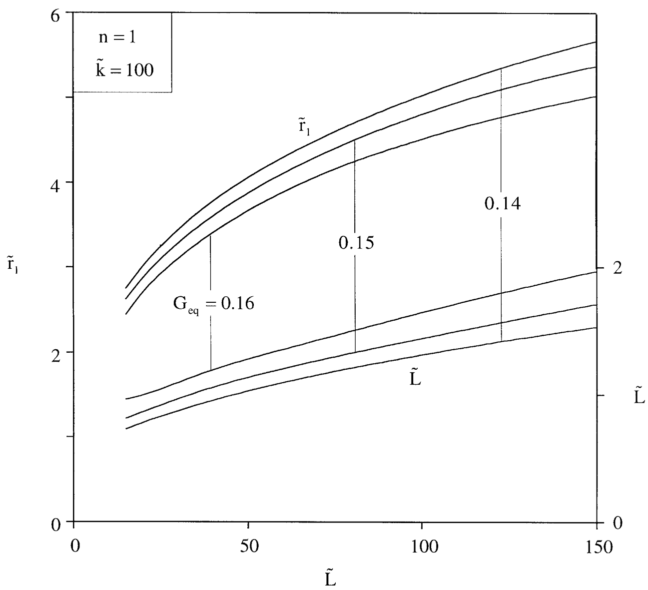

Fig. 13. The optimal geometry that corresponds to the designs optimized in Figs. 11 and 12.

The electromagnet has been optimized numerically for a fixed G_{eq} and $\widetilde{V}$, and for different numbers of high thermal conductivity discs. Fig. 14 shows how the hot spot temperature varies with the number of discs. As n increases, the hot spot temperature first drops dramatically, and then continues to decrease slowly. The optimal ratio of the volume occupied by the high thermal conductivity material is also plotted at Fig. 14. It is a slowly increasing function of n.

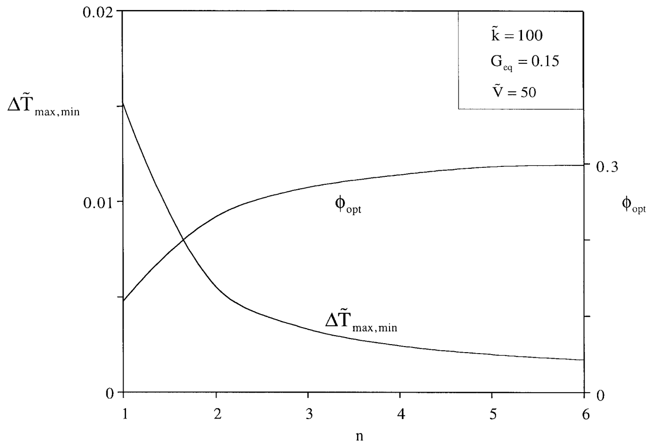

Fig. 14. The effect of the number of cooling discs on the minimized hot-spot temperature and the optimized volume fraction occupied by the discs.

8. Conclusions

In this paper we showed that the optimal shape $(\tilde{r}_1, \widetilde{L})$ and structure $(\phi,\ n)$ of an electromagnet can be deduced by considering simultaneously its thermal and magnetic functions. The optimal configuration of the system results from the competition between these two objectives, high magnetic fields and small hot-spot temperatures. For example, in order to cool the coil it is better to use greater amounts of high thermal conductivity material. On the other hand, the use of bulkier high-conductivity discs is detrimental to the magnetic performance of the electromagnet.

This competition is an opportunity to explore the optimization of architecture in a multidisciplinary domain: magnetic and thermal. The work of generating the flow architecture shows that the constructal design method can be applied to systems with more than one objective. The objectives compete not only among themselves, but also against the global constraints of the system, which are three: the highest magnetic field possible (the G parameter), the smallest volume, and the highest allowable temperature. In the first part of the paper, the volume and magnetic field efficiency were used as constraints. The alternative was to specify the maximum temperature and the coil volume, and then maximize the G parameter.

The constructal approach illustrated in this paper can be extended to more complex electromagnetic systems. The external shape of the electromagnet does not have to be a cylinder, and can be optimized as well. The same holds for the current density that, in general, can be nonuniform. Cooling methods other than high-conductivity inserts can also be studied. Finally, the list of objectives that must be pursued increases as the model becomes more practical. For example, to the thermal and magnetic objectives considered in this paper one may consider adding the maximization of the mechanical integrity [10] of the solenoid, and the minimization of the total cost of building and operating the system that employs the electromagnet. In sum, the road to a more realistic constructal design is from the local optimization of the element (e.g., electromagnet) to the "integrative" design of the installation that uses the element [11].

Acknowledgements

Louis Gosselin is grateful to the Natural Sciences and Engineering Research Council (NSERC) of Canada and to the Fonds Nature et Technologies (NATEQ) of the Province of Québec. Adrian Bejan's work was supported by a grant from the National Science Foundation.

References

[1] F. Herlach, Laboratory electromagnets—from oersted to megagauss, Physica B 319 (2002) 321–329.
[2] E.B. Haignere, W.M. Potter, Optimizing the shape and size of a uniform-current-density magnet to maximize the field at constant power, J. Appl. Phys. 47 (1976) 1657–1661.
[3] A. Miklavc, The solenoid which gives the desired value of magnetic field for the smallest possible volume of conductor, J. Appl. Phys. 45 (1974) 1680–1681.
[4] P.N. Morgan, Optimal design and construction of a lightweight minimum-power solenoid magnet, IEEE Trans. Magnetics 37 (5) (2001).
[5] A. Bejan, Constructal-theory network of conducting paths for cooling a heat generating volume, Int. J. Heat Mass Transfer 40 (1997) 799–816.
[6] A. Bejan, Shape and Structure, from Engineering to Nature, Cambridge Univ. Press, Cambridge, UK, 2000.
[7] D.J. Kroon, Electromagnetics, Philips Technical Library, Cambridge, MA, 1968.
[8] D.B. Montgomery, Solenoid Magnet Design, Wiley, New York, 1969.
[9] FIDAP Theory Manual, Vol. 7.0, Fluid Dynamics International, Evanston, IL, 1993.
[10] S. Lorente, A. Bejan, Combined 'flow and strength' geometric optimization: internal structure in a vertical insulating wall with air cavities and prescribed strength, Int. J. Heat Mass Transfer 45 (2002) 3313–3320.
[11] J.V.C. Vargas, A. Bejan, D.L. Siems, Integrative thermodynamic optimization of the crossflow heat exchanger for an aircraft environmental control system, J. Heat Transfer 123 (2001) 760–769.